Available online at www.sciencedirect.com
SCIENCE DIRECT®
International Journal of Solids and Structures 42 (2005) 1253–1268
INTERNATIONAL JOURNAL OF SOLIDS and STRUCTURES
www.elsevier.com/locate/ijsolstr

Fluid-induced vibration of composite natural gas pipelines

G.P. Zou, N. Cheraghi, F. Taheri *

Department of Civil Engineering, Dalhousie University, 1360 Barrington Street, Halifax, Nova Scotia, Canada B3J 1Z1

Received 21 July 2003; received in revised form 7 July 2004
Available online 22 September 2004

Abstract

Advancements in materials bonding techniques have led to the use of reinforced composite pipelines. The use of steel pipe with a fiber-reinforced composite over-wrap together has produced an exceptionally strong pipe with positive advantages in weight and corrosion resistively. Understanding the dynamic characteristics of this kind of sub-sea composite pipelines, which often accommodate axial flow of gas, and prediction of their response is of great interest.

This paper presents a state-variable model developed for the analysis of fluid-induced vibration of composite pipeline systems. Simply supported, clamped and clamped-simply supported pipelines are investigated. The influence of fluid's Poisson ratio, the ratio of pipe radius to pipe-wall thickness, laminate layup, the ratio of liquid mass density to pipe-wall mass density, the fluid velocity, initial tension and fluid pressure are all considered. The results of our proposed methodology are compared with those of finite element analysis, using ANSYS software.

Keywords: Composite pipes; Fluid-induced vibration; State-variable model; Ritz method

1. Introduction

The use of pipes made of composite materials for applications in oil fields has become an acceptable practice. Low to moderate pressure composite and plastic flow lines and gathering line systems for oil and natural gas have been in service for many years, but they have yet to be accepted in high-pressure natural gas transmission systems. There are a number of issues that must be overcome to make large diameter composite pipe a viable alternative in high-pressure natural gas transportation. Piping systems used for transfer of highly pressurized gas often operate under time-varying conditions imposed by pumps and

* Corresponding author. Tel.: +1 902 494 3935; fax: +1 902 484 6635.
E-mail address: farid.taheri@dal.ca (F. Taheri).

0020-7683/$ - see front matter © 2004 Elsevier Ltd. All rights reserved.
doi:10.1016/j.ijsolstr.2004.07.001

valves operations, and thus may experience severe vibration induced loading. Examples of such problems are flow-induced vibration of a pipeline supported above ground level, as well as conveying internal flow. Noteworthy investigation in this area was first made by Ashley and Haviland (1950) to describe the vibration characteristics of the Trans-Arabian pipeline. Later, Housner (1952) developed a more realistic equation to include the Coriolis effects by using Hamilton's principle. He investigated the buckling phenomenon that could occur when the flow velocity exceeds a critical value. Long (1955) first investigated clamped pipes conveying fluid. He showed experimentally that forced motions of clamped pipes, in contrast to the simply supported ones, were damped by internal flow in the range of flow velocities considered. Many studies have followed, but the principle aims of those studies were to investigate the effect of flow velocity on the natural frequencies and the critical flow velocity at which a pipe would lose its stability. The influence of the fluid pressure was first considered by Heinrich (1956). However, he considered only the special case of zero stiffness. It was not until 1966 that Gregory and Païdoussis (1966) showed that cantilever pipes could be subjected to oscillatory instabilities (flutter) rather than buckling (divergence). Benjamin (1961) proved the existence of oscillatory instabilities for a cantilever system of articulated pipes. Chen and Rosenberg (1971) appears to have been the first investigator who examined the stability of simplify supported pipes with a flow velocity which had a time dependent harmonic component superposed on the steady velocity. The divergence (buckling) critical flow velocity for a pinned-free cylinder was also determined analytically by Triantafyllou and Chryssostomidis (1984). The dynamic behaviour of long and very slender cylinders (modelled as strings, rather than beams) was also studied by Triantafyllou and Chryssostomidis (1985), among others. This work was later pursued further to investigate the dynamics of clustered cylinders in axial flow by Chen (1975), Païdoussis (1970, 1973, 1979, 2002), Gagnon and Païdoussis (1994a,b). These investigations were conducted because of the applications of such a system in tube-in-shell type heat exchangers and nuclear reactors. Additional extensions were made to deal with the dynamics of pipes containing highly annular flow (see, e.g. Païdoussis et al., 1990; Mateescu et al., 1994a,b, 1996). The linear and nonlinear dynamics of cantilevered cylindrical pipes with axial flow was investigated by Païdoussis et al. (2002). They stated that increase in flow velocity was the primary cause of loses of stability by divergence. An experimental study the interference effect on vortex-induced vibration of two side-by-side elastic cylinder, fixed at both end in a cross-flow was also presented by Wang et al. (2003). The turbulence-induced vibration of a circular cylinder in water flow with supercritical Reynolds number was experimentally studied by Koji et al. (2001). The effect of Reynolds number, fluctuating force coefficients, Strouhal number and correlation length on the vibration were evaluated. Very recently Cheng et al. (2003) proposed a novel technique to perturb interaction between vortex shedding from a bluff body and vortex-induced vibration of the body. A spectral element model for a simply supported straight pipeline conveying steady internal fluid was also presented by Lee and Oh (2003).

Another important application to be considered is the extremely long (a kilometer or longer) arrays of several parallel cylinders that host sonar sensors that are towed on the sea surface or sufficiently submerged to avoid wave induced motions. These pipe sensors pick up acoustic signals directed at, and redirected from the sea-bed strata. The accuracy of the signals, which can be affected by vibration, is of extreme importance for detaching the existence of oil or gas (see, e.g. Jan and Alexei, 2002; Didier et al., 2002).

All above-mentioned methods however have only considered pipelines made of isotropic materials, but their integrity has not been assessed and verified for pipes made of composite materials. The vibration frequencies of these pipes were obtained by the Fourier expanding method.

The present study presents details of a state-variable model developed for the analysis of fluid-induced vibration of laminated composite pipeline systems. To the knowledge of the authors the response of pipes made of composite materials under the influence of fluid velocity, initial tension and fluid pressure have not been widely explored. With the aim of contributing to the present status of our knowledgebase, we conducted a comprehensive investigation to characterize the response of such pipes subject to various parameters. Pipes having simply supported, clamped and clamped-simply supported boundary conditions

were considered. The results obtained through the proposed methodology were verified with those obtained from finite element analysis (FEA), and good comparison was obtained.

2. Derivation of composite pipe dynamic equations

The derivation is initiated by considering a representative element (P_f), with the length of dx, as shown in Fig. 1.

The fluid moves along the y-axis (see Fig. 1 for the coordinate system) with velocity of $V = \frac{\partial y}{\partial t} + U_g \frac{\partial y}{\partial x}$ inside the pipe, and the pipe itself moves in the direction y with velocity $\frac{\partial y}{\partial t}$. The kinetic energy of the system takes the form:

$$T = \frac{1}{2}\left\{\int_0^L \left(\int\int_{A_g} \rho_g \left(\frac{\partial y}{\partial t} + U_g \frac{\partial y}{\partial x}\right)^2 dA_g\, dx + \int\int_{A_w} \rho_w A_w C_a \left(\frac{\partial y}{\partial t}\right)^2 dA_w\, dx + \int\int_{A_p} \rho_p \left(\frac{\partial y}{\partial t}\right)^2 dA_p\, dx\right)\right\} \tag{1}$$

where ρ_g, ρ_p and ρ_w are the densities of the natural gas, pipe's material and sea water, respectively; $A_g = \frac{\pi}{4} D_{in}^2$, $A_w = \frac{\pi}{4} D_{out}^2$ (see Blevins, 2001; Bai et al., 2001) and $A_p = A_w - A_g$ are the cross-section areas of gas, added sea water and pipe, respectively; D_{in} and D_{out} are the inside and outside diameters of the pipe respectively (see Fig. 1); U_g is the velocity of the moving gas (in the x-direction) and C_a is the added mass coefficient (see Blevins, 2001).

The work done by the pre-tension force, which can be created by sub-sea waves can be written as

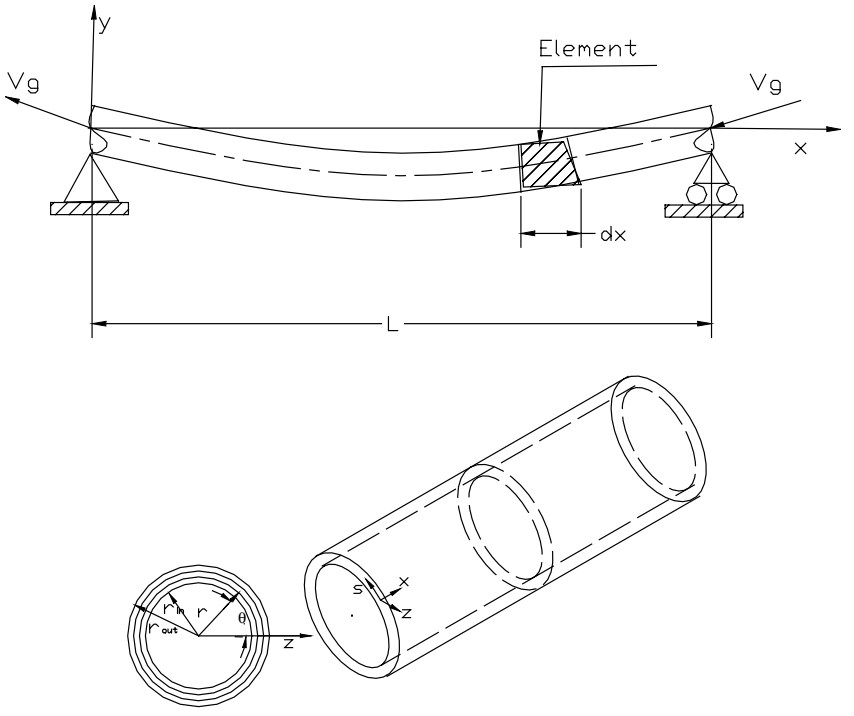

Fig. 1. A fluid-conveying pipe with pinned ends (simply supported) at sub-sea and the coordinate system.

$$\delta W_1 = \int_0^L T \frac{\partial^2 y}{\partial x^2} \delta y \, \mathrm{d}x \tag{2}$$

where T is the pre-tensioning force in the pipe.

The work done by the gas through shear friction and pressure can be expressed by:

$$\delta W_2 = -\int_0^L 2\rho_g A_g U_g^2 f \frac{L}{D_g} \frac{\partial^2 y}{\partial x^2} \delta y \, \mathrm{d}x + \int_0^L P(1 - 2v\delta) A_g \frac{\partial^2 y}{\partial x^2} \delta y \, \mathrm{d}x \tag{3}$$

where P is the gas pressure. If the downstream end is not free to flow axially, or even not completely free, internal pressurization induces an additional tensile force, which for a thin pipe is equal to $-2PvA_g$, where v is the Poisson's ratio of the pipe (Naguleswaran and Williams, 1968). Thus, the equivalent pressure can be represented in a general form as $P(1-2v\delta)A_g$, in which $\delta = 0$ signifies that there is no constraint to the axial flow of at the downstream end, otherwise $\delta = 1$. In Eq. (3) 'f' is the Fenning friction factor, which can be approximated by (Gregory and Forgarasi, 1985):

$$\frac{1}{\sqrt{f}} = -4 \log \left[\frac{k/D_g}{3.7065} + \frac{1.2613}{N_{Re}\sqrt{f}} \right], \quad N_{Re} = \frac{D_g U_g \rho_g}{\mu} \tag{4}$$

where N_{Re} is the Reynolds number, μ is the gas viscosity, k is the absolute pipe roughness and D_g is the internal diameter of the pipe.

The strain energy of the dx segment of the pipe can be represented by:

$$\Pi = \frac{1}{2} \int_0^L \Re \left(\frac{\partial^2 y}{\partial x^2} \right)^2 \mathrm{d}x \tag{5}$$

where

$$\begin{aligned} \Re &= \int_s (A_{11} y^2 + D_{11} \cos^2\theta) \mathrm{d}s \\ A_{11} &= \sum_{K=1}^{N} \left(Q_{11}^{(k)} \right) (r_k - r_{k-1}) \\ D_{11} &= \sum_{K=1}^{N} \frac{1}{3} \left(Q_{11}^{(k)} \right) (r_k^3 - r_{k-1}^3) \end{aligned} \tag{6}$$

and Q_{11} represent the stiffness terms for the composite, r_k is radius of the kth layer of cylinder. For a cylindrical pipe, $\Re$ is:

$$\Re = \pi (A_{11} \bar{r}^3 + D_{11} \bar{r}), \quad \text{where} \quad \bar{r} = (r_{in} + r_{out})/2 \tag{7}$$

Carrying out the usual steps in writing the dynamic force terms:

$$\int_{t_0}^{t_1} \delta T \, \mathrm{d}t = -\int_{t_0}^{t_1} \left\{ \int_0^L I_g \left[\frac{\partial^2 y}{\partial t^2} + 2U_g \frac{\partial^2 y}{\partial t \partial x} + U_g^2 \frac{\partial^2 y}{\partial x^2} \right] \delta y \, \mathrm{d}x + \int_0^L I_p \frac{\partial^2 y}{\partial t^2} \delta y \, \mathrm{d}x \right\} \mathrm{d}t \tag{8}$$

where

$$\begin{aligned} I_g &= \int \int_{A_g} \rho_g \mathrm{d}A_g = \rho_g A_g \\ I_p &= \int \int_{A_p} \rho_p \mathrm{d}A_p = 2\pi \int_{r_{in}}^{r_{out}} \rho^{(k)} r \, \mathrm{d}r = \sum_{k=1}^{N} \pi \rho^{(k)} (r_k^2 - r_{k-1}^2) \end{aligned} \tag{9}$$

Using the Hamilton's principle

$$\int_{t_0}^{t_1} \{\delta T - \delta \Pi + \delta W_1 + \delta W_2\}\, \mathrm{d}t = 0 \tag{10}$$

Finally, the equilibrium equation of motion for the sub-sea pipeline system can be written as:

$$\Re \frac{\partial^4 y}{\partial x^4} + \left[I_g U_g^2 + P(1-2v)A_g - T - 2I_g U_g^2 f \frac{L}{D_g} \right] \frac{\partial^2 y}{\partial x^2} + 2I_g U_g \frac{\partial^2 y}{\partial t \partial x} + (I_g + I_p + I_w) \frac{\partial^2 y}{\partial t^2} = 0 \tag{11}$$

where

$$I_w = \rho_w A_w C_a \tag{12}$$

3. The Ritz method

The inherent coupling phenomenon associated with the vibration behaviour of the pipeline system complicates the derivation of an analytical solution to the above equation. The Ritz method, an approximated method, however can be employed to solve the equation. Within this method, it is assumed that the solution of the vibration problem of the pipeline system is composed of a series of linear combination of admissible functions $\Phi_i(x/L)$, multiplied by the time-dependent generalized coordinates (Zou et al., 2003), that is:

$$y(x/L, t) = \sum_r \Phi_r(x/L) q_r(t) \tag{13}$$

where $\Phi_i(x/L)$ are the eigenfunctions of the pipeline. The general form of the eigenfunctions is given in Kelly (1993).

By substituting Eq. (13) into Eq. (11), and using the Ritz method, the following equation can be obtained:

$$[M]\{\ddot{q}\} + [G]\{\dot{q}\} + [K]\{q\} = 0 \tag{14}$$

where

$$M_{ij} = \int_0^L (I_g + I_p + I_w) \Phi_i(x/L) \Phi_j(x/L)\, \mathrm{d}x \tag{15}$$

$$G_{ij} = \int_0^L 2I_g U_g \Phi_i(x/L) \frac{\partial \Phi_j(x/L)}{\partial x}\, \mathrm{d}x \tag{16}$$

$$\begin{aligned} K_{ij} = {} & \int_0^L \Re \frac{\partial^2 \Phi_i(x/L)}{\partial x^2} \frac{\partial^2 \Phi_j(x/L)}{\partial x^2}\, \mathrm{d}x - \int_0^L I_g U_g^2 \frac{\partial \Phi_i(x/L)}{\partial x} \frac{\partial \Phi_j(x/L)}{\partial x}\, \mathrm{d}x \\ & - \int_0^L P(1-2v\delta) A_g \frac{\partial \Phi_i(x/L)}{\partial x} \frac{\partial \Phi_j(x/L)}{\partial x}\, \mathrm{d}x + \int_0^L I_g U_g^2 f \frac{L}{D_g} \frac{\partial \Phi_i(x/L)}{\partial x} \frac{\partial \Phi_j(x/L)}{\partial x}\, \mathrm{d}x \\ & + \int_0^L T \frac{\partial \Phi_i(x/L)}{\partial x} \frac{\partial \Phi_j(x/L)}{\partial x}\, \mathrm{d}x \end{aligned} \tag{17}$$

It should be noted that $[G]$ is not the conventional damping matrix; it is an unsymmetric matrix which varies according to the vibration mode.

4. State-space analysis

Solution of the above nonsymmetric equation of motion can be readily carried out by placing the equations in the state-space form. The state vector is defined to be:

$$\{\xi(t)\} = \left[\, \{q(t)\}^{\mathrm{T}} \quad \{\dot{q}(t)\}^{\mathrm{T}} \,\right]^{\mathrm{T}} \tag{18}$$

Correspondingly, the state-space form of the equations of motion is represented by:

$$[\Theta]\{\dot{\xi}\} - [\Psi]\{\xi\} = \{0\} \tag{19}$$

where

$$[\Theta] = \begin{bmatrix} [K] & [0] \\ [0] & -[M] \end{bmatrix}, \quad [\Psi] = \begin{bmatrix} [0] & [K] \\ [K] & [G] \end{bmatrix} \tag{20}$$

Note that because r is the length of each of the Ritz series, the state-space equations are a set of $2r$ coupled first-order differential equations.

Lack of symmetry in the coefficient matrix of the state vector necessitates solutions of the general left and right eigenvalue problem, such that

$$[[\Psi] - \omega_j[\Theta]]\{\varphi_j\} = \{0\}, \quad [[\Psi]^{\mathrm{r}} - \omega_j[\Theta]^{\mathrm{r}}]\{\tilde{\varphi}_j\} = \{0\} \tag{21}$$

where ω_j are the eigenvalues and the eigenvectors $\{\varphi_j\}$ and their adjoints $\{\tilde{\varphi}_j\}$ are normalized such that the bi-orthogonality conditions are satisfied such that

$$\{\tilde{\varphi}_j\}^{\mathrm{r}}[\Theta]\{\varphi_n\} = \delta_{jn}, \quad \text{and} \quad \{\tilde{\varphi}_j\}^{\mathrm{r}}[\Psi]\{\varphi_n\} = \omega_j\delta_{jn} \tag{22}$$

The eigenvalues depend on the fluid velocity because of the $[G]$. The critical speeds are the values of U_{g} at which the imaginary part of any of the minimum eigenvalues zero. The real part of the eigenvalue is related to the amount of damping exhibited by a given eigenvalue. The logarithmic decrements δ_j can be calculated by:

$$\delta_j = \frac{-2\pi \mathrm{Re}(\omega_j)}{|\mathrm{Im}(\omega_j)|} \tag{23}$$

Divergence and instabilities may be identified by searching for the speed U_{g} that induces an eigenvalue δ_j having a negative logarithmic decrements (i.e., a positive real part).

5. Examples

The results of the state-variable fluid-induced vibration method have been validated numerically for a concrete coated steel pipeline and composite pipelines with different lay ups.

5.1. Example 1: Cement coated steel pipeline

In this example, the BATS pipeline system in the Atlantic sea is considered. In this system, steel pipelines are coated by cement. The geometry and material properties are provided in Table 1, while the sub-sea properties are tabulated in Table 2. The calculated vibration results for the simply supported, cantilever and clamped-simply supported pipelines compared with the FEM results are provided in Tables 3–5, respectively. The commercial finite element program ANSYS is employed for modeling the cemented coated steel pipeline using eight node isotropic 3D solid elements (SOLID 45), with the mesh density of 20 (in the circumferential direction) × 200 (in the axial direction) × 2 (in the radial direction). Good agreements are observed from these tables. In Table 4 we also compare the results from our analytical solution

Table 1
Specifications of the cement coated steel pipe

Quantity	Symbol	Value
Geometry of pipeline		
Outside diameter	D	1.0668 m
Pipe thickness	t_s	0.0342 m
Cement coating thickness	t_c	0.030175 m
Outside diameter of cement coating	D_c	1.12776 m
Cross-section area of pipe	A	0.783844 m^2
Span length	L	59.1312 m
Material properties		
Density of steel	ρ_s	7850 kg/m^3
Density of cement	ρ_c	3043.508 kg/m^3
Density of sea water	ρ_w	1020 kg/m^3
Density of pure gas	ρ_g	2.864 kg/m^3
Density of gas content	ρ'_g	105 kg/m^3
Elastic modulus of steel	E_s	2×10^{11} N/m^2
Elastic modulus of cement	E_c	2.4×10^{10} N/m^2
Design parameters		
Design pressure	P	9.253×10^6 N/m^2
Residual tension	T	8,896 N
Content gas velocity	V	4.59 m/s
Strouhal number	S	0.2
Poisson's ratio	v	0.312
Gas viscosity	μ	0.01019744 $kg s/m^2$
Absolute pipe roughness	k/D	1×10^{-8}

Table 2
Sub-sea wave properties

Quantity	Symbol	Value
Added mass coefficient	C_a	1.0
Drag coefficient	C_D	1.45
Mean flow	$\overline{U}$	5 m/s
Amplitude of sinusoidal flow	U_m	3 m/s

Table 3
Calculated vibration frequencies of the simply supported pipeline

Mode	Structural frequency (Hz)	
	Pipe without fluid (analytical results)	Pipe without fluid (FEM results)
1	0.7382	0.72173
2	2.9526	2.9083
3	6.6435	6.5048
4	11.8106	11.565

with the FEM results for a clamped pipe that experiences and internal fluid pressure of 3 MPa. The results indicate that the first vibration frequency will be almost zero at that pressure.

In order to observe the fundamental theoretical influence of one parameter at a time (i.e., the influence of the fluid velocity, internal pressure and initial tension), when considering a parameter, the others are as-

Table 4
Calculated vibration frequencies of the clamped pipeline

Mode	Structural frequency (Hz)			
	Pipe without fluid (analytical results)	Pipe without fluid (FEM results)	Pipe with fluid pressure of 3 MPa (analytical results)	Pipe with fluid pressure of 3 MPa (FEM results)
1	0.2630	0.2587	0.0000	0.0000
2	1.6480	1.6125	1.1003	1.1194
3	4.6144	4.5395	4.0907	5.3254
4	9.0424	8.8523	8.4016	9.3538

Table 5
Calculated vibration frequencies of the clamped-simply supported pipeline

Mode	Structural frequency (Hz)	
	Pipe without fluid (analytical results)	Pipe without fluid (FEM results)
1	1.1532	1.1255
2	3.7369	3.6861
3	7.7968	7.6147
4	13.3331	13.094

sumed to be zero. Three cases were therefore considered to investigate the influence of (a) fluid velocity, (b) the internal pressure, and (c) the initial tension.

5.1.1. Case (a): Influence of the fluid velocity (while keeping $P = 0$ and $T = 0$)

The first three vibration frequencies as a functions of fluid velocities in the simply-supported, clamped and clamped-simply supported pipes were determined and are shown in Figs. 2–4, respectively. We can see from the figures that increasing fluid velocity decreases the vibration frequency of the pipeline for all considered boundary conditions. The velocity reaches to a critical value (i.e., $V/V_c = 1$, albeit a theoretical,

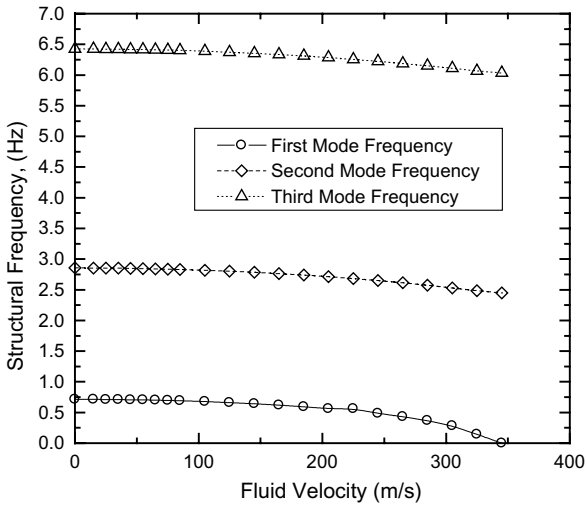

Fig. 2. Variation of the first three fundamental frequencies as a function of fluid velocities for the simply-supported pipe.

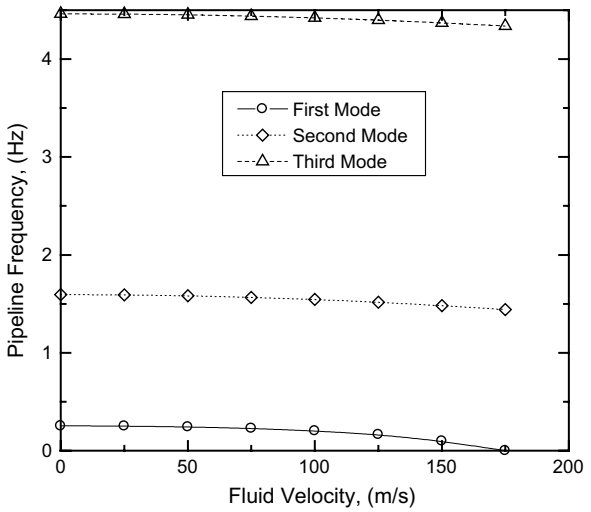

Fig. 3. Variation of the first three fundamental frequencies as a function of fluid velocities for the clamped pipe.

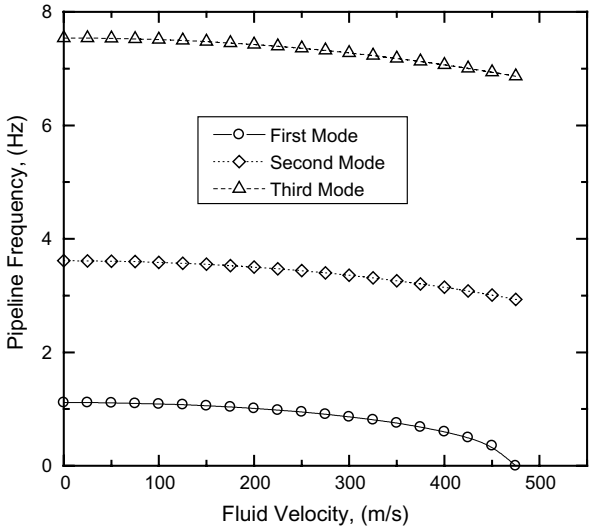

Fig. 4. Variation of the first three fundamental frequencies as a function of the fluid velocity for the cantilever-simply supported pipeline.

and not a realistic or practical value), at which the first frequency becomes zero, thus indicating that the pipe will buckle (Dodds et al., 1965). The lowest critical velocity is observed for the clamped pipe and the highest one was determined to occur for the clamped-supported pipe.

5.1.2. Case (b): Influence of the internal pressure (while keeping $V_g = 0$ and $T = 0$)

The relationship between the internal pressure and vibration frequency for the simply supported, clamped and clamped-simply supported pipes are shown in Figs. 5–7, respectively. We can see from the figures that the existence of internal pressure decreases the natural frequency of the pipe for the three

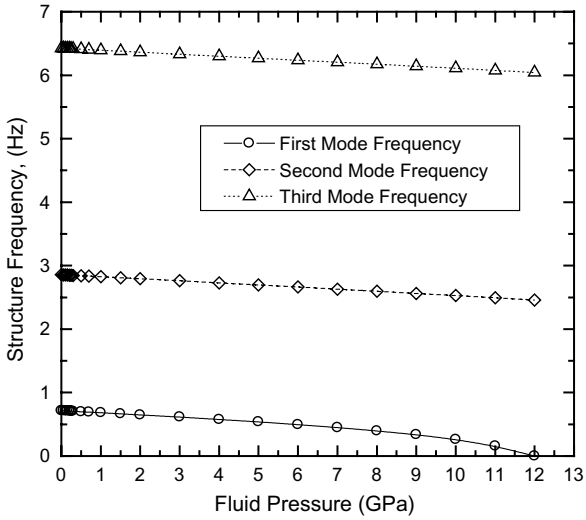

Fig. 5. Variation of the first three fundamental frequencies as a function of internal pressure (the simply-supported pipe).

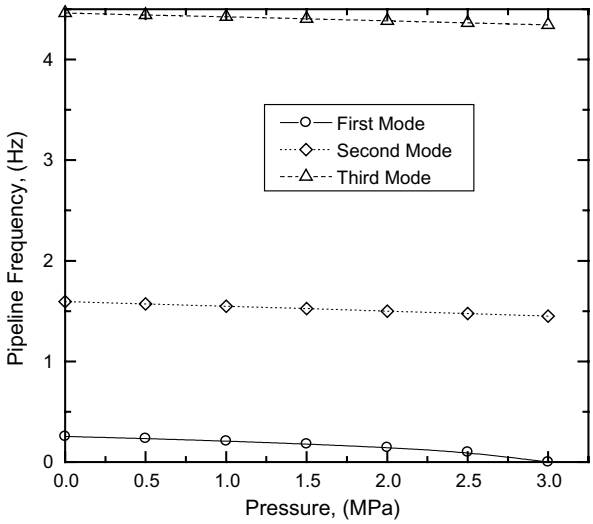

Fig. 6. Variation of the first three fundamental frequencies as a function of internal pressure (the clamped pipe).

boundary conditions. The first vibration mode frequency decreases with the increase in internal pressure P. When P reaches a certain value then the first mode frequency becomes zero ($f1 = 0$) hence buckling would prevail. The figure shows that the fluid pressure influences the vibration frequency of the clamped pipe. The internal pressure, P, causes a compressive axial force in the pipeline. If the pipeline is perfectly straight, the internal pressure would not induce a lateral force on the pipe. For pipes with any bending curvature, the existence of the force can generally aggravate the lateral bending of the pipe.

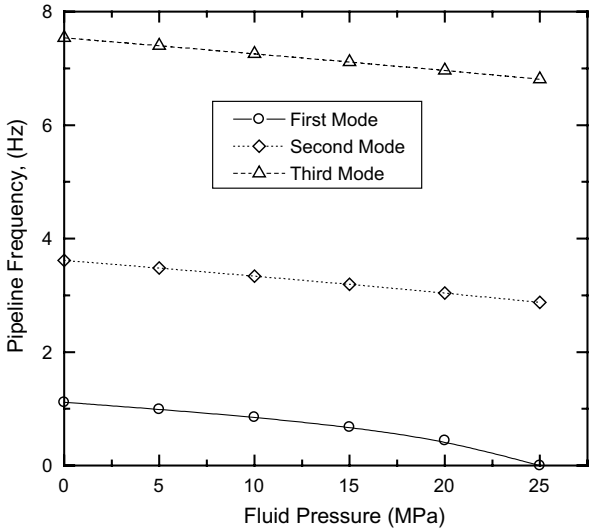

Fig. 7. Variation of the first three fundamental frequencies as a function of internal pressure (the cantilever-simply supported pipe).

5.1.3. Case (c): Influence of the pre-tensioning force (while keeping V = 0 and P = 0)

The dependency of the vibration frequency to the initial tension force or pre-tensioning force (T) of the pipes was evaluated and compared with the FEM results for all aforementioned boundary conditions, and the results are shown in Figs. 8–10, respectively. The figures show that the existence of initial tension (also called the residual tension) increases the vibration frequency of the pipeline. The commercial software ANSYS was used for this study. The model was constructed with PIPE16 element of ANSYS with 20 elements along the axial direction, simulating response of an elastic pipeline with no internal fluid, subjected only to a pretension force. It is however observed that a large pre-tensioning force (T) provides only a small increase in vibration frequency. It is therefore concluded that the notion of increasing the pre-tension force

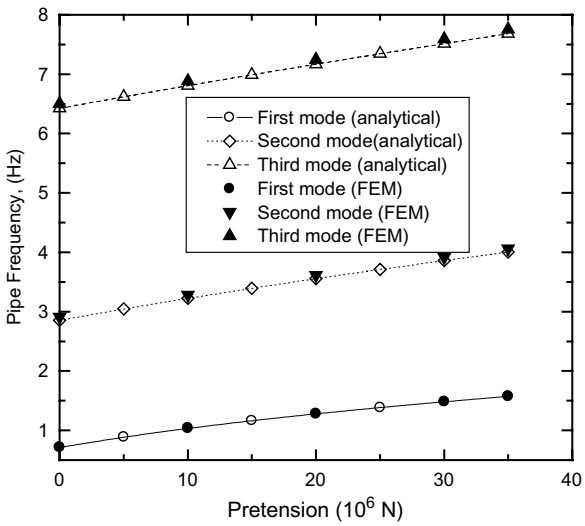

Fig. 8. Influence of pre-tensioning force on the fundamental frequencies of the simply supported pipe.

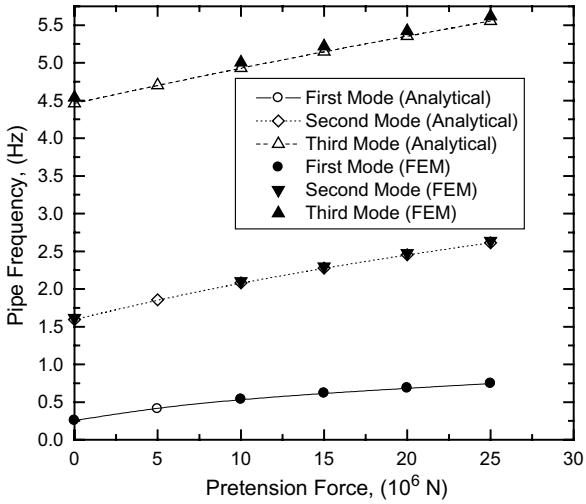

Fig. 9. Influence of pre-tensioning force on the fundamental frequencies of the clamped-simply supported pipe.

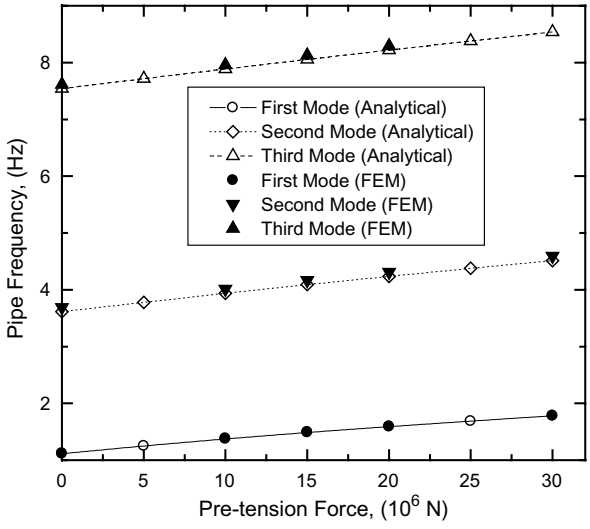

Fig. 10. Influence of pre-tensioning force on the fundamental frequencies of the clamped pipe.

to increase pipe's natural frequency is not a feasible approach. As it can be seen, a good comparison of prediction between our proposed results and the FEA results are observed.

In reality, the above-described parameters do not exist independent of one another. A pipe span is always subjected to a combination of internal pressure, pre-tension force and fluid velocity at the same time. The natural frequency is the result of superposing the influence of all these factors, including span length, mass of pipe and fluid, stiffness of the pipe, fluid velocity, internal pressure, and residual tension. In the next section, we therefore continue our investigation into influence of a combination of those parameters on the pipes' natural frequency.

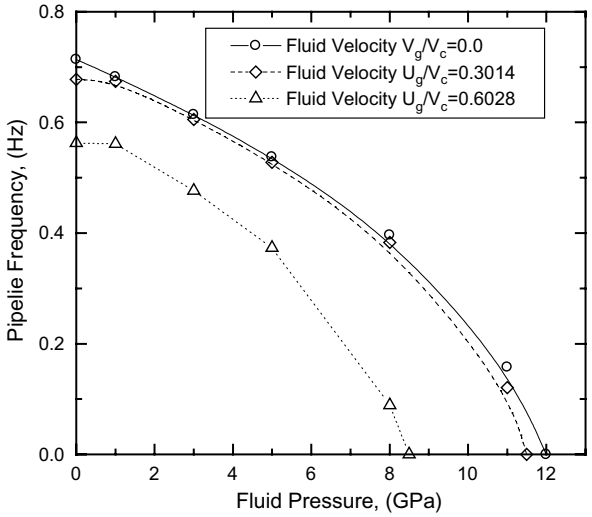

Fig. 11. Variation of pipe frequency versus internal pressure as a function of fluid velocity.

Table 6
Properties of the materials used in formation of the pipes

Layer no.	Reinforcement	E_x (GPa)	v_{xs}	G (GPa)	Ply thickness (mm)
1	1-oz polyester fiber mat	3.45	0.25	1.38	0.254
2	1.5-oz chopped strand glass mat	8.31	0.41	2.58	1.016
3	8-oz knitted glass mat.	6.21	0.15	1.83	0.559
4	19.2-oz plane woven glass mat	28.88	0.21	3.75	0.559
5	18-oz woven roving glass mat	20.68	0.15	3.28	0.610
6	28.6-oz woven roving glass mat	14.38	0.10	3.85	1.016
7	Pure epoxy resin	3.45	0.25	1.38	N/A
8	Pure vinylester resin	3.45	0.25	1.38	N/A

Table 7
Calculated vibration frequencies for a composite pipe made of fiberglass epoxy

D_0 (mm)	L (m)	Pipe wall lay up configuration (from outside to inside)			Laminate stiffness			Pipe vibration frequency (Hz)	
		#5 (mm)	#6 (mm)	#7 (mm)	$A_{11}\times10^7$ (N/m)	D_{11} (Nm)	$\Re$ (Nm^2)	No fluid	With fluid velocity $V=12$ m/s
60.22	1.30	1.98	0	2.41	5.0566	87.1528	3.4632×10^3	58.6325	52.8533
88.62	1.33	1.98	0	2.36	5.5305	90.8353	1.1855×10^4	83.5062	71.3084
114.30	5.60	2.24	0	2.21	7.6281	161.5345	2.8805×10^4	6.3814	5.1830
168.28	5.60	2.41	0	2.54	7.3630	216.7862	1.0286×10^5	9.2809	7.1555
219.08	5.60	3.25	0	2.13	5.0382	84.2246	2.9239×10^5	13.4899	9.8432
273.05	5.60	3.35	0	2.79	6.0100	125.0215	6.0356×10^5	15.9635	11.4924
323.85	5.60	1.98	1.57	2.41	8.0816	238.7322	9.2581×10^5	16.4194	11.8570

Table 8
Calculated vibration frequencies for a composite pipe made of fiberglass epoxy

D_0 (mm)	L (m)	Pipe wall lay up configuration (from outside to inside)			Laminate stiffness			Pipe vibration frequency (Hz)	
		#3 (mm)	#5 (mm)	#7 (mm)	$A_{11}\times10^7$ (N/m)	D_{11} (N m)	$\Re$ (N m^2)	No fluid	With fluid velocity $V=12$ m/s
48.08	1.29	1.34	1.46	1.98	4.6912	52.8678	1.4992×10^3	41.7439	38.8897
60.20	1.30	2.37	0.86	2.46	4.0071	54.0520	2.6615×10^3	46.5244	42.6126
88.80	1.33	1.31	1.43	2.24	4.7848	70.7234	1.0988×10^4	71.8564	63.2505
114.30	5.60	1.25	1.36	2.51	4.5534	60.9413	2.3282×10^4	5.5239	4.6222
168.28	5.60	1.49	1.63	1.98	5.2443	74.7273	8.9076×10^4	8.1425	6.4107
219.08	5.60	2.28	0.62	2.46	3.8836	84.9313	1.4799×10^5	8.4971	6.5281
273.05	5.60	2.22	1.82	2.24	6.2274	128.9144	4.6293×10^5	13.0986	9.6983
323.85	5.60	2.51	1.37	2.51	5.4167	107.9712	6.8158×10^5	14.7928	10.3971

Table 9
Calculated vibration frequencies for a hybrid polyester/glass fiber-reinforced epoxy pipe

D_0 (mm)	L (m)	Pipe wall lay up configuration (from outside to inside)				Laminate stiffness			Pipe vibration frequency (Hz)	
		#1 (mm)	#5 (mm)	#6 (mm)	#7 (mm)	$A_{11}\times10^7$ (N/m)	D_{11} (N m)	$\Re$ (N m^2)	No fluid	With fluid velocity $V=12$ m/s
48.26	1.29	0.31	3.75	0	2.84	9.0564	281.4061	2.5346×10^3	49.6973	47.4957
168.28	5.60	0.22	1.61	3.58	3.05	9.8530	535.9123	1.5809×10^5	8.0970	7.0854
273.05	5.60	0.24	0.57	4.75	2.79	9.2930	460.3722	6.8050×10^5	12.5302	10.1490
323.85	5.60	0.23	1.69	3.74	2.92	10.2120	562.5683	1.2570×10^6	15.9547	12.4526

Table 10
Calculated vibration frequencies for a hybrid polyester/glass fiber-reinforced vinylester pipe

D_0 (mm)	L (m)	Pipe wall lay up configuration (from outside to inside)					Laminate stiffness			Pipe vibration frequency (Hz)	
		#1 (mm)	#5 (mm)	#6 (mm)	#4 (mm)	#8 (mm)	$A_{11}\times10^7$ (N/m)	D_{11} (N m)	$\Re$ (N m^2)	No fluid	With fluid velocity $V=12$ m/s
47.90	1.29	0.22	1.05	0	0.96	2.08	5.8926	68.4850	1.8163×10^3	52.6998	48.2005
60.17	1.30	0	1.69	0	0.52	1.98	5.8233	76.0264	4.0184×10^3	69.7569	61.3713
88.65	1.30	0	1.98	0	0	1.98	4.8984	64.0118	1.1693×10^4	98.5970	80.6695
114.30	5.60	0	1.69	0	0	2.64	4.5305	83.0623	2.3405×10^4	6.5397	5.2569
168.28	5.60	0	2.49	0	0	2.34	6.1049	116.1515	1.0472×10^5	10.2840	7.6101
219.08	5.60	0	2.95	0	0	2.57	7.1582	173.4168	2.7385×10^5	13.6164	9.7524
273.05	5.60	0	3.48	0	0	2.13	8.1124	183.7781	6.0946×10^5	18.1741	12.2298
323.85	5.60	0	2.13	1.78	0	1.73	7.7372	188.9874	9.7909×10^5	18.8961	12.8579

5.1.4. Case (d): Influence of the combined fluid velocity and pressure

The influence of combined fluid pressure and speed ratios of $V/V_c = 0$, 0.3014 and 0.6028 for the simply supported pipe is shown in Fig. 11. It can be seen that as the fluid pressure increases, the frequency decreases and finally vanishes. At zero frequency, the system becomes unstable and buckling would occur. Under the same fluid pressure, the fluid velocity attains a larger value, as seen in Fig. 11, and the pipe's frequency decreases. In this case, the pipe can sustain a lower axial pressure thus buckling would occur.

5.2. Example 2: Influence of laminate lay up

Four different grades of centrifugally cast composite pipes were investigated. These four grades of pipes consisted of eight different reinforcement configurations as noted in Table 6. The table presents the materials' mechanical properties, densities, and nominal ply thicknesses. Various pipes were formed by combining the materials tabulated in Table 6 and their vibration characteristics were investigated by our methodology and FEM. Tables 7–10 list all dimensions, laminate stiffness A_{11} and D_{11}, the calculated vibration frequencies of pipes made of the various combinations of materials listed in Table 6, without fluid, and with fluid (gas with velocity of $V = 12\,\mathrm{m/s}$). The gas density was taken as $105\,\mathrm{kg/m^3}$ and no seawater effect was considered. The first column of each table refers to the pipes' outside diameter and the proceeding columns tabulate the pipes' length and wall configuration (with reference to the layers outlined in Table 6). The same tables tabulate the values of A_{11}, D_{11} and $\mathfrak{R}$. The important point is to realize that unlike the popular notion that the natural frequency of a pipe is a function of pipe's flexural stiffness, D_{11}, from the data and results reported in Tables 7–10 one can see that pipes' natural frequencies are indeed a function of $\mathfrak{R}$, which it is itself a function of D_{11} and A_{11}.

6. Conclusions

The Ritz method was successfully used to characterize the fluid-induced vibration of various composite pipe systems. Thin-walled composite theory was employed in developing the formulation. The formulation was developed to handle arbitrary boundary conditions. Adaptation of the model for a specific set of geometric boundary conditions requires only the selection of a suitable set of basic functions. The state-space formulation retained all fluid-pipe coupling parameters and neoconservative effects resulting from the boundary constraints. Numerical analyses were also conducted to investigate the effect of various influencing parameters, such as the fluid's velocity and pressure, pipe's pre-tensioning force and wall configuration. The results obtained based on the proposed formulation agree favorably with those obtained through finite element analysis.

Acknowledgment

The financial support of NSERC and the Atlantic Innovation Fund in the form of research grants to the third author in support of this work is gratefully acknowledged.

References

Ashley, H., Haviland, G., 1950. Bending vibrations of a pipe line containing flowing fluid. ASME Journal of Applied Mechanics 72, 229–232.

Bai, Y., Bhattacharyya, R., McCormick, M.E., 2001. Pipeline and risers. In: Elsevier Ocean Engineering Book Series, vol. 3, Elsevier Science Ltd, Oxford, UK.

Benjamin, T.B., 1961. Unstable oscillation of tubular cantilevers conveying fluid. I. Theory and II. Experiments. Proceedings of Royal Society 293 (A), 512–542.

Blevins, R.D., 2001. Flow-Induced Vibration. Krieger Publishing, Melbourne, FL, USA.

Chen, S.S., 1975. Vibration of nuclear fuel bundles. Nuclear Engineering and Design 35, 399–422.

Chen, S.S., Rosenberg, G.S., 1971. Vibration and stability of a tube conveying fluid. USAEC Report ANL-7762, Argonne National Laboratory, Argonne, IL.

Cheng, L., Zhou, Y., Zhang, M.M., 2003. Perturbed interaction between vortex shedding and induced vibration. Journal of Fluids and Structures 17 (7), 887–901.

Didier, B., Graham, W., Laurent, D., 2002. Nuggets: demonstrating the use of flexible flowlines as an alternative to traditional thinking in subsea pipeline systems. Pipes and Piplines International 47 (4), 17–26.

Dodds, H.L. Jr., Harry, L.R., 1965. Effect of high-velocity fluid flow on the bending vibrations and static divergence of a simply supported pipe. National Aeronautics and Space Administration Report NASA TN D-2870.

Gagnon, J.O., Païdoussis, M.P., 1994a. Fluid coupling characteristics and vibration of cylinder clusters in axial flow. Part I: Theory. Journal of Fluids and Structures 8, 257–291.

Gagnon, J.O., Païdoussis, M.P., 1994b. Fluid coupling characteristics and vibration of cylinder clusters in axial flow. Part II: Experiments. Journal of Fluids and Structures 8, 293–324.

Gregory, G.A., Forgarasi, M., 1985. Alternate to standard friction equation. Oil and Gas Journal 1 (April), 124–127.

Gregory, R.W., Païdoussis, M.P., 1966. Unstable oscillation of tubular cantilevers conveying fluid, I. Theory and II Experiments. Proceedings of the Royal Society 293 (A), 512–542.

Heinrich, G., 1956. Vibrations of tubes with flow. Zeitschrift für Angewandte Mathematik und Mechanik 36 (11/12), 417–429.

Housner, G.W., 1952. Bending vibrations of a pipe line containing flowing fluid. ASME Journal of Applied Mechanics 19, 205–209.

Jan, J., Alexei, T., 2002. Implementation of ISO-14000 standards in routine environmental of oil and gas fields by means of GIS and remote sensing. Journal of Canadian Petroleum Technology 41 (9), 11–15.

Kelly, S.G., 1993. Fundamentals of Mechanical Vibrations. McGraw-Hill, NY, USA.

Koji, I., Masaki, M., Takaaki, S., Akira, Y., Kenji, O., 2001. Evaluation of turbulence-induced vibration of a circular in supercritical Reinolds number flow. JSME International, Series B: Fluids and Thermal Engineering 44 (4), 721–728.

Lee, U., Oh, H., 2003. The spectral element model for pipelines conveying internal steady flow. Engineering Structures 25 (8), 1045–1055.

Long Jr, R.H., 1955. Experimental and theoretical study of transverse vibration of a tube containing flowing fluid. ASME Journal of Applied Mechanics 22 (1), 65–68.

Mateescu, D., Païdoussis, M.P., Belanger, F., 1994a. Unsteady annular viscous flows between oscillating cylinders. Part I: Computational solutions based on a time-integration method. Journal of Fluids and Structures 8, 489–507.

Mateescu, D., Païdoussis, M.P., Belanger, F., 1994b. Unsteady annular viscous flows between oscillating cylinders. Part II: A hybrid time-integration solution based on azimuthal Fourier expansions force configurations with annular back steps. Journal of Fluids and Structures 8, 509–527.

Mateescu, D., Mekanik, A., Païdousis, M.P., 1996. Analysis of 2-D and 3-D unsteady annular flows with oscillating boundaries, based on a time-dependent coordinate transformation. Journal of Fluids and Structures 10, 57–77.

Naguleswaran, S., Williams, C.J.H., 1968. Lateral vibration of a pipe conveying a fluid. Journal Mechanical Engineering Science 10 (3), 228–238.

Païdoussis, M.P., 1970. Dynamics of submerged towed cylinders. Eighth Symposium on Naval Hydrodynamics: Hydrodynamics in the Ocean Environment. Ocean of Naval Research, US Department of the Navy ARC-179, pp. 981–1016.

Païdoussis, M.P., 1973. Dynamics of cylindrical structures subjected to axial flow. Journal of Sound and Vibration 29, 365–385.

Païdoussis, M.P., 1979. The dynamics of clusters of flexible cylinders in axial flow: theory and experiments. Journal of Sound and Vibration 65, 391–417.

Païdoussis, M.P., 2002. Fluid–Structure Interactions: Slender Structures and Axial Flow, vol. 2. Academic Press, London.

Païdoussis, M.P., Mateescu, D., Sim, W.G., 1990. Dynamics and stability of a flexible cylindrical narrow coaxial cylindrical duct subjected to annular flow. Journal of Applied Mechanics 57, 232–240.

Païdoussis, M.P., Grinevich, E., Adamovic, D., Semler, C., 2002. Linear and nonlinear dynamics of cantilevered cylinders in axial flow. Part 1: Physical dynamics. Journal of Fluids and Structures 16 (6), 691–713.

Triantafyllou, G.S., Chryssostomidis, C., 1984. Analytic determination of the buckling speed of towed slender cylindrical beams. ASME Journal of Energy Resources Technology 106, 246–249.

Triantafyllou, G.S., Chryssostomidis, C., 1985. Stability of a string in axial flow. ASME Journal of Energy Resources Technology 107, 421–425.

Wang, Z.J., Zhou, Y., So, R.M.C., 2003. Votex-induced vibration characteristics of two fixed-supported elastic cylinders. Journal of Fluids Engineering, Transactions of ASME 125 (3), 551–560.

Zou, G.P., Naghipour, M., Taheri, F., 2003. A nondestructive method for evaluating natural frequency of glued-laminated beams reinforced with GRP. Journal of Nondestructive Testing and Evaluation 19 (1–2), 53–65.